ISSN 1063-7834, Physics of the Solid State, 2016, Vol. 58, No. 1, pp. 19–24. © Pleiades Publishing, Ltd., 2016.
Original Russian Text © S.S. Aplesnin, O.B. Romanova, A.I. Galyas, V.V. Sokolov, 2016, published in Fizika Tverdogo Tela, 2016, Vol. 58, No. 1, pp. 21–26.

SEMICONDUCTORS

Study of Electrical and Thermoelecrical Properties of Sulfides $Tm_xMn_{1-x}S$

S. S. Aplesnin[a,b], O. B. Romanova*[a,b], A. I. Galyas[c], and V. V. Sokolov[d]

[a] *Kirensky Institute of Metals, Siberian Branch of the Russian Academy of Sciences, Akademgorodok 50–38, Krasnoyarsk, 660036 Russia*

[b] *Reshetnikov Siberian Aerospace University, pr. imeni Gazety "Krasnoyarskii Rabochii" 31, Krasnoyarsk, 660014 Russia*

[c] *Scientific–Practical Materials Centre, National Academy of Sciences of Belarus, ul. P. Brovki 19, Minsk, 220072 Belarus*

[d] *Institute of Inorganic Chemistry, Siberian Branch of the Russian Academy of Sciences, pr. Akademika Lavrent'eva 3, Novosibirsk, 630090 Russia*

**e-mail: rob@iph.krasn.ru*

Received June 2, 2015

Abstract—Variable-valence $Tm_xMn_{1-x}S$ ($0 \leqslant x \leqslant 0.15$) compounds have been synthesized and their structural, electrical, and thermoelectrical properties have been studied in the temperature range of 80–1100 K. The regions of existence of solid solutions of sulfides $Tm_xMn_{1-x}S$ with the NaCl-type fcc lattice have been determined. It has been found that, as thulium ions are substituted for manganese cations, the electrical resistivity increases, and the lattice parameter increases more sharply than that corresponding to the Vegard's law. The study of the temperature dependences of the thermopower coefficient has revealed that the current carrier sign is retained to 500 K for all the substitution concentrations, and the charge carrier type changes from the hole type to the electron type with variations in the temperature. The experimental data have been explained in terms of the exciton model.

DOI: 10.1134/S1063783416010029

1. INTRODUCTION

Compounds containing chemical rare-earth elements with variable valence such as Sm, Yb, Ce, Eu, and Tm have a number of unique properties. As external conditions (temperature, pressure, and composition) are changed, they often undergo phase transitions having a purely electron nature and related with the change in filling of $4f$ electron levels [1]. Simultaneously, the magnetic properties are also changed [2] (localized magnetic moments disappear); i.e., the transitions are the magnetic–nonmagnetic state transitions [3]. Manganese sulfide doped with samarium [4] and gadolinium [5] ions demonstrates the change in the conduction type from the semiconductor to metallic conduction and significant magnetoresistance (on an order of 100%) in the paramagnetic region at room and higher temperatures [6].

Thulium sulfide has a cubic crystal structure with the lattice parameter 5.412 Å. This compound is characterized by metallic-type conduction at $T > 100$ K with an electron concentration of 10^{22} cm^{-3} and resistivity of 10^{-6} Ω cm at room temperature [7]. Thulium, whose electron configuration of the $4f$ shell is almost filled and unstable, can form compounds with other elements and be in states Tm^{2+} ($4f^{13}$, term $^2F_{7/2}$) and Tm^{3+} ($4f^{12}$, term $^3H_6$). In TmS, thulium ion is in the trivalent state with the filling $n_f = 0.65$ of the $4f$ level; the difference between energies of divalent and trivalent states is 0.3 eV [8]. The proximity between the energies of thulium in various states leads to TmS demonstrating the Kondo effect, at which the band electrons are grouped around thulium ions and screen its magnetic moment [9]. Under pressure, "quasi-localized" states are expanded and transit to the conduction band, which is manifested as a transition to the usual metallic state. This is confirmed by the pressure dependence of the thermopower of thulium that decreases at pressures up to 20 GPa and ceases to change at higher pressures [10].

It is known that, in $Re^{3+}X$-type compounds, europium, samarium, ytterbium, and, to a lower degree, thulium chalcogenides exhibit anomalously large interatomic distances against a smooth background with varying lattice parameters (lanthanide compression). This fact is explained by the existence of REM ions in these compounds in the Re^{2+} state (or a near state); the corresponding ions have larger ionic radii, which is observed as the increase in the lattice param-

eter. The main anomalous properties of these states are related to the position of the f level near the Fermi level E_F, namely, with the existence of a narrow resonance level immediately at the Fermi surface. The electronic phase transition is also observed in thulium chalcogenides, where the divalent state is less stable. At normal pressure, thulium is divalent in TmTe, trivalent in TmS [11] and has a variable valence in TmSe. In this case, the valence of Tm in TmTe and TmSe is changed under action of pressure. The Tm_xS compounds exhibit the properties typical of Kondo systems such as compounds with variable valence and Kondo lattices [11]. In particular, the Hall effect in Tm_xS has an anomalous character; the Hall coefficient increases as temperature decreases and reaches values much higher than those in the normal metals [12] as a result of the scattering of conduction electrons by ions with localized magnetic moment.

The valence transition in variable-valence compounds, according to theoretical calculations [13], is related to the hybridization of wave functions of the 4*f* and 5*d* states. The transition evolution can follow two scenarios: one of them is related to the formation of excitons; the hole is at the 4*f* level, and the electron is localized in the vicinity of the hole. According to another model, the electron transits to the *d* band, and a heavy-fermion metal forms. The experiments performed on SmS and TmSe with pressure applied indirectly confirm the exciton state [14]. As pressure increases, the 4*f* level intersects the conduction band bottom, which is accompanied by a change in the volume at constant resistance. Further increase in pressure leads to a sharp change in the resistance. The manganese ion radius is significantly smaller than the thulium ion radius, and the value of hybridization of 3*d*–4*f* ions Mn–Tm is also lower than that of the 5*d*–4*f* ions Tm–Tm. Because of this, as manganese is replaced with thulium, excitons can form at the interface between clusters of thulium ions in the manganese sulfide matrix.

Monosulfide α-MnS is an second-type antiferromagnet with Néel temperature $T_N = 150$ K; it has a face-centered cubic (fcc) lattice of the NaCl type [15, 16]. Manganese monosulfide is a *p*-type semiconductor with low hole mobility in narrow (~0.5 eV) 3*d* bands, charge carrier concentration $n \sim 10^{-18}$ cm^{-3}, and the conduction activation energy in the paramagnetic state $E_a \sim 0.3$ eV [17]. The conduction provided by electrons lying below the Fermi level in the t_{2g} and e_g bands has a hole character, which is confirmed by the measurements of the thermopower and the Hall effect [18–20].

TmS and MnS compounds have the same NaCl-type crystal lattice, and the homogeneity region of $Tm_xMn_{1-x}S$ solid solutions is 20%. In the fcc lattice, the critical percolation concentration of magnetic rare-earth ions is $x_c = 2/z = 2/12 = 0.17$, where z is the number of the nearest neighbors. As the concentration of the substitution of thulium ions for manganese ions increases in the vicinity of the critical concentration, the resistivity can sharply decrease and the current carrier type can be changed (from holes to electrons) if electrons will transit from the 4*f* level to the 3*d* band. In the opposite case, as excitons form at the Mn–Tm boundary, the resistivity will increase. The validity of choosing the mechanism of the electron transition in the $Tm_xMn_{1-x}S$ compounds is confirmed by the measurements of the resistivity and the thermopower coefficient at various temperatures.

2. SAMPLES, EXPERIMENTAL TECHNIQUE, AND RESULTS

The synthesis of $Re_xMn_{1-x}S$ is described in detail in [19]. We briefly consider the specific features of synthesizing the $Tm_xMn_{1-x}S$ system. The charge for melting and crystallizing the melt was prepared by a careful mixing of the calculated amounts of a polycrystalline manganese sulfide prepared by sulfidization of analytically-pure manganese dioxide and a polycrystallinethulium monosulfide produced as a result of interaction of lithium hydride and one-and-half thulium sulfide for compositions with thulium concentrations of 0.01 and 0.1 atomic fraction with respect to cations. Te compositions with thulium concentrations $x = 0.15$, 0.10, 0.05, and 0.01 were prepared using a powder of crystals of stoichiometric one-and-half thulium sulfide. The crystallization was carried out from temperatures of 1600°C. No sublimation was observed; because of this the crystal composition was not different from the charge. The completeness of sulfidation was controlled by X-ray phase analysis and the weight method.

The X-ray diffraction of sulfides $Tm_xMn_{1-x}S$ ($0.01 \leqslant x \leqslant 0.15$) was studied using a DRON-3 diffractometer with CuK_α radiation at a temperature of 300 K after their synthesis and the measurements of their transport properties. The X-ray diffraction patterns measured after the measurement performed show that all the materials have stable crystal states to temperatures of 1100 K. The X-ray diffraction shows that the compounds synthesized are single-phase and have the NaCl-type fcc structure typical of manganese monosulfide. As the degree of cation substitution x increases, unit cell parameter a increases linearly, which indicates the formation of $Tm_xMn_{1-x}S$ solid solutions (Fig. 1). The increase in the lattice parameter as compared to a linear increase according to the Vegard's law seems to be due to the localization of electrons at the interface between Mn and Tm ions and a weak hybridization of the 4*f*–3*d* orbitals that is described by the exponential dependence on the distance.

The resistivity and the thermopower coefficient $\alpha(T)$ were measured in the temperature range of 80–1100 K by two probes in the equipment, whose struc-

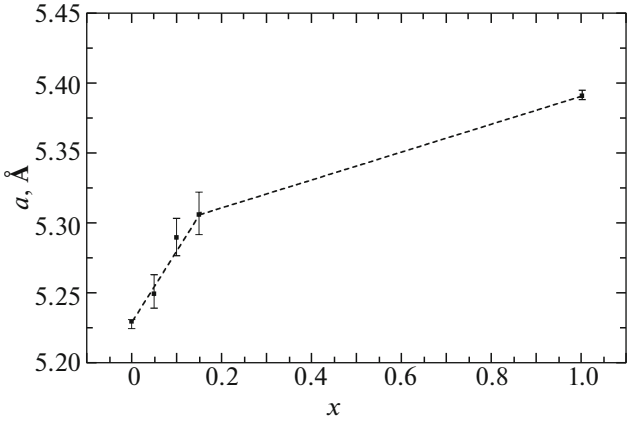

Fig. 1. Concentration dependence of lattice parameter a of solid solutions $Tm_xMn_{1-x}S$.

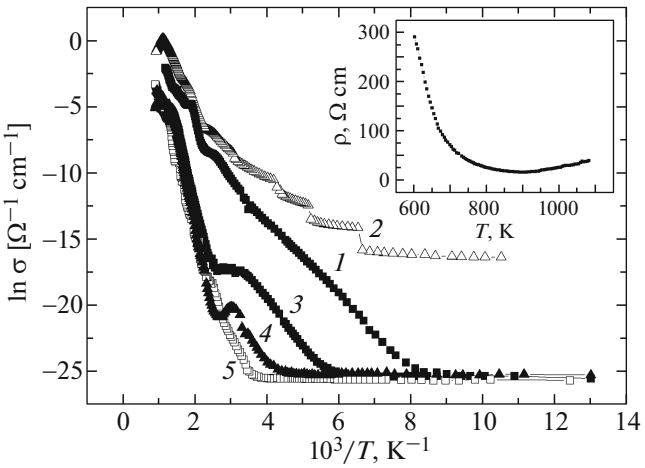

Fig. 2. Temperature dependence of the conductivity for the samples of the $Tm_xMn_{1-x}S$ system with concentration x = (*1*) 0, (*2*) 0.01, (*3*) 0.05, (*4*) 0.1, and (*5*) 0.15. The insert shows the temperature dependence of the resistivity at high temperatures for the composition with $x = 0.01$.

ture and operation principle were described in [21]. The equipment makes it possible to measure the resistance and the thermopower continuously without changing the sample.

Figure 2 shows the electrical conductivity of $Tm_xMn_{1-x}S$ solid solutions. Dependences $\ln\sigma(10^3/T)$ are characteristic of materials with semiconductor conductivity. At low temperatures, the temperature dependence of conductivity of the composition with $x = 0.01$ can be represented as three steps observed at $T = 151$, 188, and 240 K. It should be noted that insignificant increase in the conductivity in the vicinity of the Néel temperature are also observed for the compositions $x = 0.05$ at $T = 135$ K and $x = 0.1$ at $T = 132$ K. These compositions also demonstrate low maxima in dependences $\sigma(T)$ at 92 K for $x = 0.05$ and at 102 and 180 K for $x = 0.1$. The conductivity of composition $x = 0.15$ also exhibits jumps within 3–6% at temperatures $T = 112$, 170, 192 K. A sharp increase in the conductivity is observed at temperatures $T = 170$ K for $x = 0.05$, $T = 215$ K for $x = 0.1$, and $T = 270$ K for $x = 0.15$. The activation energy was found from the slope tangent of the linear part of dependence $\lg\rho(1/T)$ in the range 180 K $< T <$ 320 K; the activation energy increases from 0.2 eV for composition with $x = 0.05$ to 0.4 eV for $x = 0.1$. In the temperature range of 320–420 K, as seen from dependence $\ln\sigma(10^3/T)$, the conductivity is almost independent of temperature for concentrations $x = 0.05$ and 0.1, and its behavior is characteristic of impurity semiconductors. At temperatures higher than 500 K, the activation energy increases to 1.03 eV for $x = 0.05$ and to 1.1 eV for $x = 0.1$.

Insignificant doping of the $Tm_{0.01}Mn_{0.99}S$ sample with thulium ions brings about an increase in the conductivity and the appearance of jumps in temperature dependence $\ln\sigma(10^3/T)$. Temperature dependence of the resistivity of this composition (insert in Fig. 2) has a minimum at $T = 880$ K, and the resistivity increases with increasing temperature to 1100 K. For $x = 0.05$, at high temperatures, dependence $\sigma(T)$ has a minimum at $T = 790$ K and a maximum at $T = 880$ K. For $x = 0.1$, a minimum is observed at $T = 790$ K and a low maximum at $T = 820$ K. The existence of the maxima at the temperature dependence of the conductivity at high temperatures can be due to the scattering of electrons at the 4*f* level. All the samples are characterized by a highohmic state even at room temperature (as compared to the resistivity observed in manganese monosulfide [22]). As the substitution concentration of a rare-earth metal in the MnS lattice increases, the resistance increases (from 200 kΩ for $x = 0.01$ to 280 GΩ for $x = 0.15$).

The current carrier sign was found from the temperature dependence of the thermopower coefficient α measured in the temperature range of 300–1100 K for the $Tm_xMn_{1-x}S$ solid solutions with concentration $0 \leqslant x \leqslant 0.15$ (Fig. 3). The absolute value of coefficient α decreases as the thulium content in the $Tm_xMn_{1-x}S$ solid solutions increases. In $Tm_{0.01}Mn_{0.99}S$, the thermopower coefficient is positive over the entire temperature range under study and indicates hole-type conduction (Fig. 3b). The thermopower has two maxima for the composition with $x = 0.05$ at $T = 400$ and 840 K (Fig. 3c). In $Tm_{0.1}Mn_{0.9}S$, the thermopower coefficient decreases during heating and changes its sign in the temperature ranges of 500–600 K and 870–1040 K (Fig. 3d). The sign of α of the compound with $x = 0.15$ is negative at $T > 500$ K, except the range 580 K $< T <$ 750 K (Fig. 3e). This indicates the predominantly electron type of conduction. Similar behavior is observed in $Re_xMn_{1-x}S$ (*Re* = Gd, Yb) [1, 20].

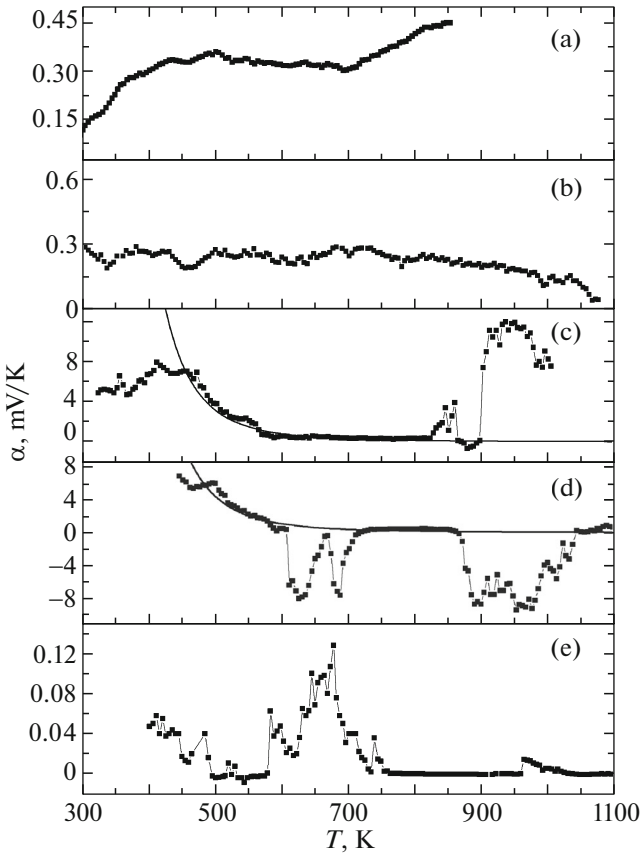

Fig. 3. Temperature dependence of the thermopower coefficient for the samples of the $Tm_xMn_{1-x}S$ system with concentration x = (a) 0, (b) 0.01, (c) 0.05, (d) 0.1, and (e) 0.15. For compositions x = (c) 0.05 and (d) 0.1 in the temperature range of 450–600 K, the thermopower coefficient is described by the pair concentration ($\alpha \sim N_{ex} = \exp(-E_{ex}/k_BT)$, where E_{ex} = 0.3 eV) and shown by the solid line.

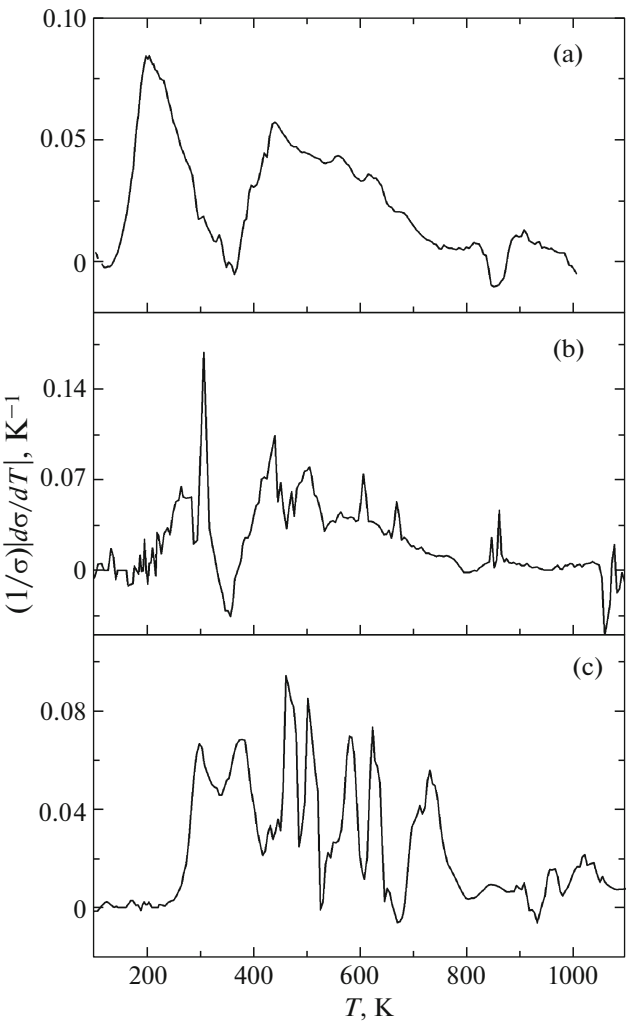

Fig. 4. Temperature dependence of the relative change in the conductivity $(1/\sigma)|d\sigma/dT|$ for compositions x = (a) 0.05, (b) 0.1, and (c) 0.15.

3. DISCUSSION OF THE RESULTS

The mechanism of appearance of the thermopower in semiconductors in the paramagnetic region is provided by the electrons being carried away by phonons. The interaction between holes and long-wave acoustic phonons brings about power dependence $\alpha(T) \sim T^{-3.5}$ [23] that is observed in semiconductors at low temperatures (50–100 K). The interaction between holes and optical phonons is substantial at higher temperatures, and the number of such phonons in the vibration spectrum decreases exponentially $n_{ph} \sim \exp(-h\omega_0/k_BT$ at $k_BT < h\omega_0/4$. The relaxation time of a charge carrier on the optical mode is inversely proportional to the number of phonons ($\tau \sim 1/n_{ph}$); because of this, we can expect an exponential dependence for the thermopower $\alpha(T) = A\exp(h\omega_0/k_BT)$ [24]. The experimental data obtained for the compositions with x = 0.05 and 0.1 are not described by this dependence. Another mechanism is related to the current carriers: electrons or holes.

The temperature gradient leads to the formation of a diffusion electron current with the current density $j = Dq|dn/dl| = Dq|dn/dT|(1/l)(dl/dT)l = Dql(|dn/dT|)(1/\beta)$, where D is the electron diffusion coefficient; q is the electron charge; l is the sample length; and β is the thermal expansion coefficient of the sample. We represent the potential difference in a closed circuit in the case as there is a temperature gradient in the form $U = El = j\rho l = l^2\rho qD(|dn/dT|)(1/\beta)$. In our samples, the electrical resistance is mainly determined by the current carrier concentration $\rho \sim 1/n$, and the value of the thermopower is $\alpha \sim (1/n)|dn/dT| = (1/\sigma)|d\sigma/dT|$. The relative change in the conductivity with temperature $(1/\sigma)|d\sigma/dT|$ is shown in Fig. 4; the temperatures of the maxima coincide with the temperatures of the thermopower extremes, except high temperature $T >$ 900 K. This difference seems to occur as a result of the fact that the conductivity is due to the change in the current carrier concentration. At high temperatures,

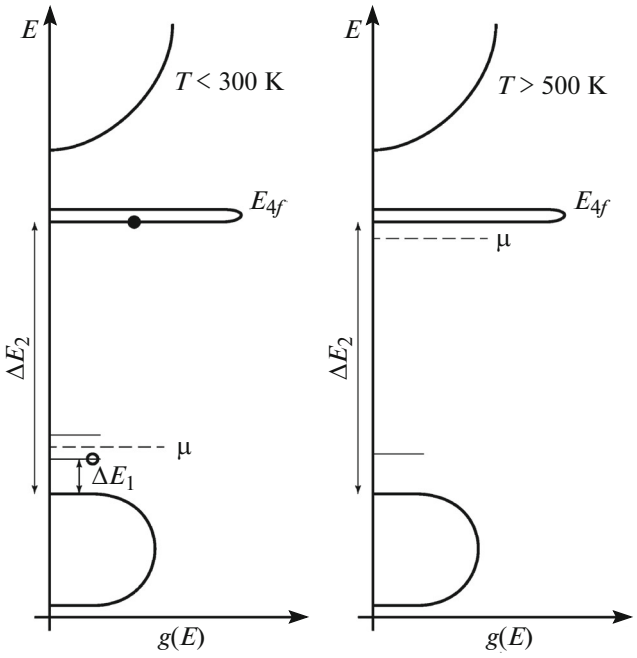

Fig. 5. Electronic structure of the $Tm_xMn_{1-x}S$ system. On the ordinate the energy is plotted; the abscissa is the density of electronic states $g(E)$. E_{4f} is the 4*f*-level energy; μ is the chemical potential; ΔE_1 is the energy difference between the acceptor level and the valence band top; ΔE_2 is the energy difference between the donor level (that is split by the crystal field(thin lines)) and the valence band top. The dark circle shows an electron, and the bright circle shows a hole.

the conductivity is changed within 5–20%; it is a result of the scattering of current carriers by electrons localized at the 4*f* level. The jumps in the temperature behavior of the resistivity and the thermopower can be explained in the model of bounded electron–hole pairs. The substitution of thulium for manganese forms an excess electron charge that is compensated by the arrangement of sulfur ions in interstitial sites. An analysis of the chemical composition at a local area several micrometers in size using an electron microscope indicates a sulfur excess of 0.035 atoms/mol for the composition with $x = 0.1$ and 0.045 atoms/mol for $x = 0.15$. In the $Tm_xMn_{1-x}S$ solid solutions, the chemical phase separation forms; excess sulfur ions with hole-type conduction form at the surface of thulium ion clusters; i.e., the electron–hole transition occurs. To explain the kinetic properties of the $Tm_xMn_{1-x}S$ solid solutions, we consider the electronic structure depicted in Fig. 5 that shows the positions of chemical potential μ with respect to the valence band and the conduction band, and also the position of the donor (impurity) level E_{4f} corresponding to 4*f* electrons of thulium laying below the conduction band bottom. Figure 5 also shows the energy difference between the acceptor level and the valence band top ΔE_1 and the energy difference between the donor level and the valence band top ΔE_2. Sulfur atoms are in the interstitial sites and can be interpreted as acceptors with an energy level near the valence band top. At $T = 166$ K, the lattice parameter of manganese sulfide has a kink accompanying by a jump in the conductivity for plane (111) and the decrease in the activation energy from 0.2 to 0.02 eV [25]. At temperature $T = 125$ K, which is lower than the Néel temperature, the rhombohedral distortion is observed [22]. The substitution of thulium for manganese shifts the temperatures of the structural lattice deformations, splits acceptor levels, and, correspondingly, the conductivity over the acceptor level is changed. As temperature increases, the transitions of electrons from the valence band on the acceptor level prevails at $T > 160$–200 K, which leads to the increase in the conductivity in the valence band. Above 300 K, the impurity states are saturated (become filled), and the conductivity is almost independent of temperature. Further heating induces the recombination of electron–hole pairs and the shift of the chemical potential to the 4*f* energy level. The annihilation of the pairs leads to equalizing the potentials at the Tm–Mn interface, and the temperature dependence of the thermopower coefficient in the range of 450–600 K is described well by the concentration of electron–hole pairs: $\alpha \sim N_{ex} = \exp(-E_{ex}/k_BT)$ with energy $E_{ex} = 0.3$ eV, where E_{ex} is the energy of interaction between electron and hole. Figure 3 shows this dependence with the solid line. The minima in the temperature dependence of the resistivity and the extremes in the case of the thermopower at $T > 900$ K are due to the intersection of the chemical potential level and the 4*f* level.

4. CONCLUSIONS

We synthesized new antiferromagnetic semiconductor sulfide compounds with a variable valence, i.e., $Tm_xMn_{1-x}S$ ($0 \leqslant x \leqslant 0.15$), which have the NaCl-type fcc lattice. It was found that the resistivity of the compounds increases as manganese is replaced by variable-valence thulium ions. There are two temperature ranges in which the activation energy of $Tm_xMn_{1-x}S$ differs by several times. At high temperatures, the minimum in the temperature dependence of the resistivity and the extreme values of the thermopower coefficient are observed for all compositions, except $x = 0.15$. The current carrier type is changed from the hole to electron type in the compositions with $x \geqslant 0.1$ in some concentration range. In $Tm_xMn_{1-x}S$ with substitution concentrations $x \geqslant 0.1$, the thermopower value decreases as compared to that of manganese sulfide. The thermopower mechanism is related to the current carriers, and the temperatures of the anomalies of the resistivity and thermopower coincide. We proposed a model of coupled electron–hole states with the dissociation energy at a temperature that qualitatively explains the experimental results.

ACKNOWLEDGMENTS

This study was supported by the Russian Foundation for Basic Research (project no. 15-42-04099 r_sibir_a) and State Contract no. 114090470016.

REFERENCES

1. S. S. Aplesnin, O. B. Romanova, A. M. Khar'kov, and A. I. Galyas, Phys. Solid State **57** (5), 886 (2015).
2. S. S. Aplesnin, A. M. Harkov, E. V. Eremin, O. B. Romanova, D. A. Balalev, V. V. Sokolov, and A. Yu. Pichugin, IEEE Trans. Magn. **47**, 4413 (2011).
3. D. I. Khomskii, Sov. Phys.—Usp. **22** (10), 879 (1979).
4. S. Aplesnin, O. Romanova, A. Harkov, D. Balaev, M. Gorev, A. Vorotinov, V. Sokolov, and A. Pichugin, Phys. Status Solidi B **249**, 812 (2012).
5. O. B. Romanova, L. I. Ryabinkina, V. V. Sokolov, A. Yu. Pichugin, D. A. Velikanov, D. A. Balaev, A. I. Galyas, O. F. Demidenko, G. I. Makovetskii, and K. I. Yanushkevich, Solid State Commun. **150**, 602 (2010).
6. S. S. Aplesnin and M. N. Sitnikov, JETP Lett. **100** (2), 95 (2014).
7. A. V. Golubkov, E. V. Goncharova, V. P. Zhuze, G. M. Loginov, V. M. Sergeeva, and I. A. Smirnov, *Physical Properties of Rare-Earth Chalcogenides* (Nauka, Leningrad, 1973) [in Russian].
8. P. Strange, A. Svane, W. M. Temmerman, Z. Szotek, and H. Winter, Nature (London) **399**, 756 (1999).
9. J. Derr, G. Kneel, B. Sake, M.-A. Méasson, and J. Flouquet, J. Phys.: Condens. Matter **18**, 2089 (2006).
10. M. N. Abdusalyamova, P. A. Alekseev, E. S. Klement'ev, E. V. Nefedova, and V. I. Nizhankovskii, Phys. Solid State **36** (1), 79 (1994).
11. B. M. Buttaev, A. V. Golubkov, T. B. Zhukova, M. V. Romanova, V. V. Romanov, V. M. Sergeeva, and I. A. Smirnov, Sov. Phys. Solid State **32** (8), 1367 (1990).
12. B. M. Butaev, A. V. Golubkov, A. V. Gol'tsev, and I. A. Smirnov, Sov. Phys. Solid State **33** (12), 2030 (1991).
13. K. A. Kikoin and A. S. Mishchenko, J. Exp. Theor. Phys. **77** (5), 828 (1993).
14. O. B. Tsiok, L. G. Khvostantsev, A. V. Golubkov, I. A. Smirnov, and V. V. Brazhkin, Phys. Rev. B: Condens. Matter **90**, 165141 (2014).
15. D. J. Vaughan and J. R. Craig, *Mineral Chemistry of Metal Sulfides* (Cambridge University Press, Cambridge, 1978; Mir, Moscow, 1981).
16. G. A. Petrakovskii, S. S. Aplesnin, G. V. Loseva, L. I. Ryabinkina, and K. I. Yanushkevich, Sov. Phys. Solid State **33** (2), 233 (1991).
17. S. J. Youn, B. I. Min, and A. J. Freeman, Phys. Status Solidi B **241**, 1411 (2004).
18. J. B. Goodenough, *Magnetism and the Chemical Bond* (Wiley, New York, 1963; Metallurgiya, Moscow, 1968).
19. S. S. Aplesnin, L. I. Ryabinkina, O. B. Romanova, V. V. Sokolov, A. Yu. Pichugin, A. I. Galyas, O. F. Demidenko, G. I. Makovetskii, and K. I. Yanushkevich, Phys. Solid State **51** (4), 698 (2009).
20. A. I. Galyas, O. F. Demidenko, G. I. Makovetskii, K. I. Yanushkevich, L. I. Ryabinkina, and O. B. Romanova, Phys. Solid State **52** (4), 687 (2010).
21. G. I. Makovetskii, A. I. Galyas, O. F. Demidenko, K. I. Yanushkevich, L. I. Ryabinkina, and O. B. Romanova, Phys. Solid State **50** (10), 1826 (2008).
22. S. S. Aplesnin, L. I. Ryabinkina, G. M. Abramova, O. B. Romanova, N. I. Kiselev, and A. F. Bovina, Phys. Solid State **46** (11), 2067 (2004).
23. F. J. Blatt, *Physics of Electronic Conduction in Solid* (McGraw, New York, 1968).
24. S. S. Aplesnin, L. V. Udod, M. N. Sitnikov, D. A. Velikanov, M. V. Gorev, M. S. Molokeev, A. I. Galyas, and K. I. Yanushkevich, Phys. Solid State **54** (10), 2005 (2012).
25. L. I. Ryabinkina, S. S. Aplesnin, G. A. Petrakovskii, G. M. Abramova, N. I. Kiselev, and O. B. Romanova, Solid State Commun. **129**, 195 (2004).

Translated by Yu. Ryzhkov